Molecular cloning and multifunctional characterization of GRIM-19 (gene associated with retinoid-interferon-induced mortality 19) homologue from turbot (*Scophthalmus maximus*)

Na Wang [a,1], Xianli Wang [b,1], Changgeng Yang [c,1], Xiaojie Zhao [d], Yuxi Zhang [e], Tianzi Wang [a], Songlin Chen [a,*]

[a] Yellow Sea Fisheries Research Institute, Chinese Academy of Fishery Sciences, Qingdao 266071, China
[b] Sarite Center for Stem Cell Engineering Translational Medicine, East Hospital, Stem Cell Research Center, Tongji University School of Medicine, Shanghai 200120, China
[c] Key Laboratory of Freshwater Biodiversity Conservation and Utilization of Ministry of Agriculture, Yangtze River Fisheries Research Institute, Chinese Academy of Fishery Sciences, Wuhan 430223, China
[d] Weifang Marine Environment Monitoring Central Station of State Oceanic Administration, Weifang 261041, China
[e] Qingdao Agricultural University, Qingdao 266109, China

ARTICLE INFO

ABSTRACT

GRIM-19 (gene associated with retinoid-interferon-induced mortality 19), a novel cell death regulatory gene, plays important roles in cell apoptosis, embryogenesis, mitochondrial respiratory chain and immune response. To date, little information is known about fish GRIM-19 characteristics except orange-spotted grouper (*Epinephelus coioides*). Here a new GRIM-19 gene is identified and characterized from turbot (*Scophthalmus maximus*), an economic marine fish in China and Europe. Briefly, turbot GRIM-19 is a 595-bp gene encoding a 144 amino acids protein, which shares the closest relationship with Atlantic halibut (*Hippoglossus hippoglossus*). The expression of turbot *grim-19* in liver, spleen and kidney is up-regulated by the infection of *Vibrio anguillarum* and LCDV (lymphocystis disease virus). Subsequently, a recombinant protein of turbot GRIM-19 is acquired and the anti-bacterial function is proved by liquid culture inhibition experiment. The subcellular location indicates that turbot GRIM-19 is co-localized with STAT3 in the cytoplasm, which is mainly determined by GRIM-19 41–84 amino acids and STAT3 1–321 amino acids. Finally, the involvements of turbot GRIM-19 in cell apoptosis and NF-κB pathway are investigated. All these data help to understand GRIM-19 function in fish, as well as provide the application possibility of GRIM-19 in fish disease resistance breeding.

© 2013 Elsevier Ltd. All rights reserved.

1. Introduction

GRIM-19 (gene associated with retinoid-interferon-induced mortality 19) is a cell death regulatory gene (Angell et al., 2000) originally identified in the process of tumor cells death induced by interferon-β (IFN-β) and retinoic acid (RA) (Moore et al., 1994; Lindner et al., 1997). Overexpression of GRIM-19 enhances the cells sensitivity to IFN-RA-induced death, while the introduction of antisense GRIM-19 mRNA confers growth advantage to cells (Angell et al., 2000). The function of GRIM-19 involved in tumor cell death is partly linked with its capability to bind and suppress the activity of STAT3 (signal transducer and activator of transcription 3) (Lufei et al., 2003; Zhang et al., 2003). Given the constitutive expression of STAT3 in various tumors and cancer cell lines (Bromberg et al., 1999; Yu et al., 2009), GRIM-19 has become an appropriate candidate for molecular cancer therapy (Zhang et al., 2008; Máximo et al., 2008; Fan et al., 2012).

GRIM-19 is also essential for early embryonic development because homology deletion of GRIM-19 in mice causes lethality at embryonic day 9.5 (Huang et al., 2004). Meanwhile, as a functional component of mitochondrial complex I (the NADH dehydrogenase 1 alpha subcomplex subunit 13, NDUFA13), GRIM-19 is necessary for mitochondrial respiratory chain complex I assembly and the electron transfer activity (Huang et al., 2004; Lu and Cao, 2008; Fearnley et al., 2001).

Besides its involvements in the apoptosis, embryogenesis and mitochondrial respiratory chain, GRIM-19 also participate in pathology and immune response (Seo et al., 2002; Barnich et al., 2005; Zhou and Amar, 2006; Chen et al., 2012). The viral proteins such as vIRF1 protein of kaposi's sarcoma-associated herpes virus

HHV-8 and E6 protein of human papillomavirus HPV-16 could inhibit cell death by interacting with GRIM-19 (Seo et al., 2002). In human intestinal epithelial cells infected with *Salmonella typhimurium*, GRIM-19 could activate NF-κB (nuclear factor-kappa B) pathway by interacting with NOD2 (nucleotide-binding oligomerization domain containing 2) and control pathogen invasion (Barnich et al., 2005). The heterogeneous GRIM-19$^{+/-}$ mice is prone to spontaneous urinary tract infection by *Staphylococcus saprophyticus* with reduced bacterial killing ability of macrophages (Chen et al., 2012).

To date, little information is known about fish GRIM-19 characteristics except orange-spotted grouper (*Epinephelus coioides*) (Shi et al., 2013). And the function of GRIM-19 in fish immune response and apoptosis remains to be discovered. Turbot, an importantly economic marine fish in China and Europe, is suffering from serious diseases caused by *Vibrio anguillarum*, LCDV (lymphocystis disease virus), VHSV (viral hemorrhagic septicemia virus), TRBIV (turbot reddish body iridovirus) and so on (Chen et al., 2005; Nishizawa et al., 2006; Shi et al., 2004). Aiming at turbot disease resistance breeding, GRIM-19 is an important candidate gene for study.

In present study, based on the part cDNA sequences of GRIM-19 (Meng et al., 2009), the full-length cDNA and genomic DNA of turbot GRIM-19 were cloned and characterized. Further, the involvements of GRIM-19 in immune response and apoptosis are investigated. Subsequently, GRIM-19 recombinant proteins are purified for the detection of anti-bacterial ability. Finally, the possible interaction of GRIM-19 with STAT3 (Wang et al., 2011) and NF-κB are also explored by subcellular location and luciferase assay.

2. Material and methods

2.1. Fish and cell line

Turbots weighing about 100 g were obtained from Haiyang aquatic company of Yantai and every six turbots were raised in a 72 L breeding tank with running seawater at 16 °C. The TK cell line, derived from turbot kidney (Wang et al., 2010), was cultured in Eagle's minimal essential medium (MEM) (Gibco) supplemented with 10% fetal bovine serum (FBS) (Gibco) at 24 °C. The EPC (epithelioma papulosum cyprinid cell line) (Fijan et al., 1983) was maintained in MEM supplemented with 10% FBS at 25 °C.

2.2. Sample preparation and RNA isolation

For gene cloning and tissue expression pattern analysis, 11 tissues including liver, intestine, muscle, skin, heart, brain, spleen, kidney, head kidney, fin and gill were collected from three individuals, respectively. As well as, 50 turbot embryos of multi-cells stage, blastula stage, gastrula stage, somites stage, heart-beating stage, larva stage and alevin stage were harvested, respectively.

In order to analyze the expression pattern of GRIM-19 under pathogen infection, 7×10^6 CFU (colony forming units) *V. anguillarum* or 10 TCID$_{50}$ (50% tissue culture infective dose) LCDV suspensions or physiological saline (PS, NaCl solution with 0.9% concentration) per turbot were injected intraperitoneally as described (Wang et al., 2011). Three pathogen-injected fishes were anaesthetized at 6, 12, 24, 48, 72 and 96 h post injection, respectively. Tissues including liver, spleen and kidney were collected and kept at liquid nitrogen until use. In addition, these three tissues taken from PS-injected fishes at 12 h after injection were used as the control.

Total RNA was extracted from above samples using Trizol reagent (Invitrogen) according to the manufacturer's instructions.

2.3. The cloning of turbot GRIM-19 cDNA and genomic DNA

Based on the 362 bp partial sequence of turbot GRIM-19 cDNA retrieved from turbot spleen cDNA library (Meng et al., 2009), primers GRIM19-51 (5′-GGTGGTTCTTAAACGTACCA-3′), GRIM19-52 (5′-GCTCCTCGCGGGGCCGGAGG-3′), GRIM19-31 (5′-GACTTTCGGGATACAGCATG-3′) and GRIM19-32 (5′-GGTGTTTGGTTACTGGAGGC-3′) were designed for the 5′ and 3′ RACE using the BD SMART™ RACE cDNA amplification kit (BD Biosciences Clontech). In brief, the first strand cDNA synthesis for 5′ and 3′ RACE was performed on liver-derived RNA with primers OligodG, 5′-CDS and 3′-CDS, respectively. To obtain the 5′ fragment, primers GRIM19-51/UPM and GRIM19-52/NUP were used for the primary PCR and the nested PCR respectively. Similarly, the 3′ fragment of GRIM-19 was obtained by nested PCR with primers GRIM19-31/UPM and GRIM19-32/NUP. PCR products were subcloned into pMD-18T vector and sequenced by ABI 3730 DNA Analyzer. Finally, the 5′ and 3′ fragments, together with above 362 bp sequence, were joined into the entire GRIM-19 cDNA, which was further confirmed by PCR amplification by primers GRIM19_1 (5′-ACGCGGGGAGGAGGAAGATG-3′) and GRIM19_2 (5′-ACAGAAAAAGAAAGTTTAAT-3′) within the predicted 5′ and 3′ UTR, respectively.

Based on the obtained GRIM-19 cDNA sequences, primers GRIM19D-N1(5′-AAGCGAAACCTTCCGAAAGGACGAC-3′), GRIM19D-C1(5′-GATGCCGATCCCAATGCCGAAC-3′), GRIM19D-N2(5′-ACGCAGATTGAGGACCTGGAAGCC-3′) and GRIM19D-C2(5′-GACTGCAAGCTGAATTGAGTGAGCG-3′) were further designed to acquire its genomic DNA sequences. These two products were sub-cloned into pMD-18T vector, sequenced by ABI 3730 DNA Analyzer and joined into the entire turbot GRIM-19 genomic DNA.

2.4. The phylogenetic tree construction

The deduced turbot GRIM-19 amino acids sequence was submitted into the BLAST program (http://blast.www.ncbi.nlm.nih.gov) in search of its counterpart sequences. Multiple sequences alignment was performed with the ClustalX program. Then an unrooted phylogenetic tree was constructed by the neighbor-joining (NJ) algorithm of MEGA 5.05 program (Tamura et al., 2011) based on the sequences alignment. The phylogenetic tree was tested for reliability by 1000 bootstrap replications.

2.5. The recombinant expression, identification and anti-bacterial ability of GST-GRIM19 fusion protein

In order to obtain the recombinant protein of turbot GRIM-19, its coding sequence (CDS) amplified by TGRIM19+E (5′-ATAGAATTCATGGCGGGGTCCAAGGTGA-3′) and TGRIM19−X (5′-CAGCTCGAGTTAAACGTACCACAAGAAGC-3′) was firstly sub-cloned in pGEX-4T-1 to construct pGEX-GRIM19. Then, the expression of the GST-tagged fusion protein was induced with pGEX-GRIM19 by 1 mM isopropyl-b-D-thiogalactopyranoside (IPTG) at 37 °C for 1, 2, 3, 4, 5, 6, 7, 8, 18 and 24 h. As well as, pGEX-4T-1 was used as the control. All the collected samples were subjected to 12% SDS–PAGE discontinuous vertical electrophoresis. The BandScan software was used to analyze the fusion protein content.

In further, Western-blotting was carried out to verify the GST-GRIM19 protein. The mouse monoclonal antibody against GST and HRP labeled sheep anti-mouse IgG were used as the detection and conjugated antibody, respectively. The membrane was colored by the DAB Horseradish Peroxidase Color Development Kit (Beyotime).

For the purification of GST and GST-GRIM19 fusion protein, 1 L LB medium of pGEX-4T-1 and pGEX-GRIM19 induced by IPTG at 37 °C for 7 h were collected and broken by ultrasonic wave. The GSTrap™ FF column was used for the purification follow as the

protocol. Then the purified proteins were treated with ToxinEra-serTM Endotoxin Removal Kit (Genscript) and dialyzed with dialysis tube (Solarbio).

Finally, the purified GST-GRIM19 fusion and GST protein was resolved with the concentration of 50 ng/μl and 100 ng/μL. In addition, the GST-IGF-I protein (Zhao et al., 2010) was used for the negative control. The anti-bacterial activity was analyzed with liquid culture inhibition method. Briefly, 100 μl *V. anguillarum* (10^6 CFU in 2216E medium) and 100 μl GST-GRIM19, GST-IGF-I or GST proteins were mixed in a 96 well plate at 28 °C for 24 h. The mixture was taken out and coated on 2216E plate for the colony number counting at 24 h. Every group was repeated for three times.

2.6. The subcellular location analysis

In order to analyze the subcellular location of turbot GRIM-19, primers GFP19C+E (AGCGAATTCATGGCGGGGTCCAAGGTG), GFP 19C−B (AGCGGATCCTAAGTTTCTTCGATCTTG), GFP19N+E (AGCGA ATTCATGGGCATCATGGTGTTTG) and GFP19N−B (AGCGGATCCAA CGTACCACAAGAAGC) were designed to amplify the corresponding cDNA of ΔN region (41–144 amino acids), ΔN1 region (85–144 amino acids) and ΔC region (1–84 amino acids) of GRIM-19. Then, three fragments were ligated into pEGFP-N3 (BD Biosciences Clontech) with EcoRI/BamHI to construct pGFP-GRIM19-ΔN, pGFP-GRIM19-ΔN1 and pGFP-GRIM19-ΔC (Fig. 8A).

In order to determine the co-localization of turbot GRIM-19 and STAT3 (Wang et al., 2011), pGFP-STAT3 and pCS2-GRIM19-Cherry were constructed with primers GPFS3+H (5′-ACGAAGCTTATGGCTC GGTGGAACCAGTTGCAG-3′), GFPS3−E (5′-ACGGAATTCCGCATAGGC GATGCTACATCCATGTC-3′), CherryG9+H (5′-ACGAAGCTTATGGCGG GGTCCAAGGTG-3′), CherryG9−C (5′-ACGATCGATAACGTACCACAA-GAAGC-3′) based on pEGFP-N3 and pCS2tfe3Cherry (a kind gift from Professor Yunhan Hong of National University in Singapore) with restriction enzymes sites HindIII/EcoRI and HindIII/ClaI.

Also, the DNA sequences related to the ΔN (322–784 amino acids) and ΔC (1–321 amino acids) region of STAT3 amplified with primers GFPS3+H (5′-ACGAAGCTTATGGCTCGGTGGAACCAG TTGCAG-3′), GFPS3−E1 (5′-ACGGAATTCCGCGCACTCTTCATCAGGT TT-3′), GFPS3+H2 (5′-ACG AAGCTTATGTTTGTGGTGGAACGACAGC C-3′) and GFPS3−E (5′-ACG GAATTCCGCATAGGCGATGCTACATCCA TGTC-3′) were sub-cloned into pEGFP-N3 vector to construct pGFP-STAT3-ΔN and pGFP-STAT3-ΔC (Fig. 8A).

Turbot TK cells were chosen for cell transfection assay in present study. The cell transfection was carried out in 12-well plates by Lipofectamine 2000 (3 μl: 1 μg) follow as the protocol. At 36 h after transfection, the cells were rinsed with PBS for 5 min, fixed with 4% paraformaldehyde for 15 min, rinsed again with PBS for 5 min, treated with 0.1% Triton X-100 for 5 min, and stained with DAPI (100 ng/ml) for 10 min.

All treated samples was observed and captured under Nikon ECLIPSE TE 2000-U fluorescence microscope.

2.7. Cell apoptosis assay

In order to explore the function of GRM-19 in cell apoptosis, primers 3G19N+E (5′-AGCGAATTCATGGGCATCATGGTGTTTG-3′), 3G19N−X (5′-AGCCTCGAGAACGTACCACAAGAAGC-3′), 3G19C+E (5′-AGCGAATTCATGGCGGGGTCCAAGGTG-3′) and 3G19C−X (5′-AGCCTCGAGTAAGTTTCTTCGATCTTG-3′) were designed for construction of p3.1-GRIM19 (1–144 amino acids), p3.1-GRIM19△N (41–144 amino acids) and p3.1-GRIM19△C (1–84 amino acids) based on the vector pcDNA3.1 (+) with restriction enzymes sites EcoRI/XhoI.

The cell apoptosis function of GRIM-19 was detected in TK and EPC cells with Annexin V-FITC Apoptosis Detection Kit (Beyotime). Briefly, pcDNA3.1, p3.1-GRIM19, p3.1-GRIM19△N or p3.1-GRIM19△C was transfected into 24 well plates with each well of 0.6 μg and 2 μl Lipofectamine 2000 (Invitrogen) by three replicates. After 36 h transfection, 100 μl 10^3 TCID50/ml LCDV was introduced into each well. The treated cells were harvested into the centrifuge tube by trypsin digestion at 24 h after virus infection. Then, 500 μl Binding Buffer, 5 μl Annexin V-FITC and 5 μl PI was successively added into $1\sim5 \times 10^5$ cells precipitates. Finally, the cells apoptosis was detected by BD FACSCalibur flow cytometer (BD Biosciences) after 10 min dark incubation.

2.8. The luciferase assay

The plasmids pcDNA3.1/p3.1-GRIM19/△N/△C, pNFκB-Luc and phRL-TK were co-transfected in 24 well plates with each well of 0.3 μg: 0.3 μg: 0.03 μg and 2 μl Lipofectamine 2000 (Invitrogen) by three replicates. After 36 h transfection, 100 μl 10^3 TCID50/ml LCDV was introduced into each well. After 24 h infection, Firefly and Renilla luciferase activites were measured using the Dual-Luciferase Reporter Assay System (Promega). Briefly, 100 μl 1× PLB (Passive Lysis Buffer) was added into each well and 20 μl cell lysate was transferred into the luminometer tube containing 100 μl LAR II. The value of Firefly luciferase was firstly measured on a Promega GloMax™ 20/20 Luminometer (E5311), then Renilla luciferase activity was detected after the addition of 100 μl Stop & Glo Reagent. Finally, the relative luciferase activities were obtained by dividing the Firefly luciferase activity by the Renilla luciferase activity.

2.9. Statistical analysis

The results were analyzed by a one-way analysis of variance (ANOVA). The values were expressed as mean ± SD in the figures. Differences between treatments were detected with the Student–Newman–Keuls (SNK) generated by SPSS 11.5.

3. Results

3.1. Isolation and sequence analysis of GRIM-19

Based on the 362 bp partial cDNA of GRIM-19 from turbot spleen cDNA library, two fragments with lengths of 460 and 493 bp were obtained by 5′ and 3′ RACE, respectively. After splicing and assembling analysis by Vector NTI 11.5, these three fragments were joined into turbot GRIM-19 full-length cDNA with 595 bp which contained a 17 bp 5′UTR, a 435 bp open reading frame (ORF) encoding 144 amino acids and a 143 bp 3′UTR. The complete nucleotide and deduced amino acids sequences of turbot GRIM-19 (Genbank Number: DQ400688 and ABD61722) are shown in Fig. 1.

Turbot GRIM-19 encodes a putative protein of 144 amino acids with a predicted molecular mass of 17 kD and theoretical isoelectric point (pI) of 9.64. SMART analysis indicated the existence of Pfam GRIM-19 domain between 2 and 131 amino acids.

Turbot GRIM-19 genomic DNA were further acquired by lengths of 3359 bp with five exons and four introns (FJ617007). By comparison of GRIM-19 genomic sequences in several species (Fig. 2), the exon–intron organization of turbot GRIM-19 is similar to that of human (*Homo sapiens*), mouse (*Mus musculus*), cattle (*Bos taurus*) and pig (*Sus scrofa*) GRIM-19. While, there are different exons numbers in southern house mosquito (*Culex quinquefasciatus*), fruit fly (*Drosophila melanogaster*) and western gorilla (*Gorilla gorilla*) GRIM-19 with two, three and four exons, respectively.

```
1     acgcggggaggaggaagATGGCGGGGTCCAAGGTGAAGCAGGACATGCCTCCTCTGGGGAG
1                      M  A  G  S  K  V  K  Q  D  M  P  P  L  G
61    GCTATGCGGCGTTCGATTACAAGCGAAACCTTCCGAAAGGACGACTTTCGGGATACAGCA
15     G  Y  A  A  F  D  Y  K  R  N  L  P  K  G  R  L  S  G  Y  S
121   TGTTCGGCATTGGGATCGGCATCATGGTGTTTGGTTACTGGAGGCTATTTAAGTGGAACA
35     M  F  G  I  G  I  G  I  M  V  F  G  Y  W  R  L  F  K  W  N
181   GAGAGAGGAGGCGCCTCCTGATTGAGGACCTGGAAGCCAGGATAGCTATGATGCCTCTGC
55     R  E  R  R  R  L  L  I  E  D  L  E  A  R  I  A  M  M  P  L
241   TGCAAGCAGAGCAAGATCGAAGAAACTTACGAATGCTGAGGGAAAATTTAGAAGAGGAGG
75     L  Q  A  E  Q  D  R  R  N  L  R  M  L  R  E  N  L  E  E  E
301   CGATTGTCATGAAGGACGTTCCAGGTTGGAAGGTCGGTGAGAGCGTCTTCCACACGGACC
95     A  I  V  M  K  D  V  P  G  W  K  V  G  E  S  V  F  H  T  D
361   GCTGGGTCGCCCCTATGACAGAGGAGCTGTTCAACCTCCGGCCCCGCGAGGAGCTTTTGC
115    R  W  V  A  P  M  T  E  E  L  F  N  L  R  P  R  E  E  L  L
421   ACAAGCGTTTTGGCTTCTTGTGGTACGTTTAAgaaccaccgagatgaagagtcctgagct
135    H  K  R  F  G  F  L  W  Y  V  *
481   cttccaccttccacagacacatcaagtggaacaagcgctcactcaattcagcttgtaaa
541   tgttcaaaattaaactttctttttctgtaaaaaaaaaaaaaaaaaaaaaaaaaaa
```

Fig. 1. The cDNA and deduced amino acid sequences of turbot GRIM-19. The open reading frame sequences are shown in capital letters. The initiation codon (ATG) and the termination codon (TAA) are shown in bold format. The polyadenylation signal (AATTAAA) in the 3-untranslated regions is underlined.
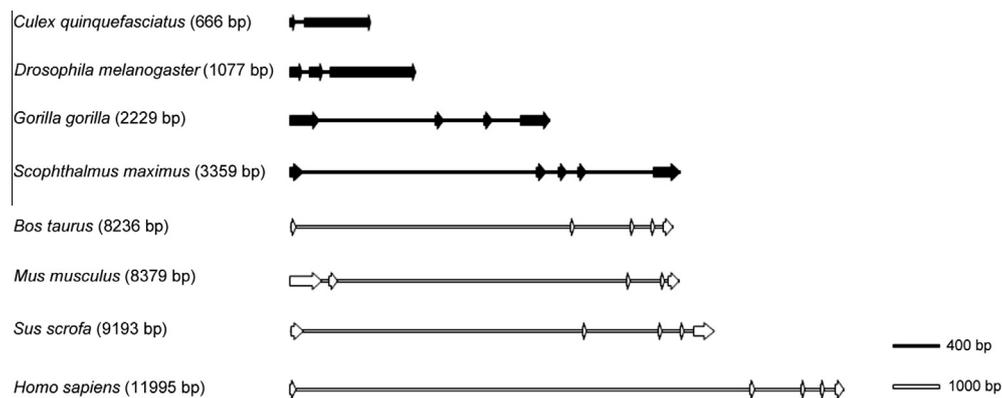

Fig. 2. Comparison of GRIM-19 genomic sequences structures. Turbot and other 7 species GRIM-19 genomic sequences are displayed: southern house mosquito *Culex quinquefasciatus* (NW_001886709), fruit fly *Drosophila melanogaster* (NC_004354), western gorilla *Gorilla gorilla* (NC_018443), turbot *Scophthamus maximus* (FJ617007), cattle *Bos taurus* (AC_000164), mouse *Mus musculus* (NC_000074), pig *Sus scrofa* (NC_010444), human *Homo sapiens* (NC_000019). The bold arrows show exons, and the connecting lines show introns.

3.2. The phylogenetic tree analysis

After submission of turbot GRIM-19 deduced amino acids sequence into BLAST program, 26 GRIM-19 or NDUFA13 proteins were acquired and used for the phylogenetic tree construction with the neighbor-joining method (Fig. 3). Turbot GRIM-19 protein shared the closest relationship with Atlantic halibut (*Hippoglossus hippoglossus*) GRIM-19. All fish and frog GRIM-19 homologues were clustered into one group. The other group contained higher vertebrate GRIM-19. Another group is the invertebrate GRIM-19 including southern house mosquito (*C. quinquefasciatus*) and silkworm (*Bombyx mori*).

3.3. Expression profiles of grim-19 in tissues and embryogenesis

To determine the distribution of turbot *grim-19* transcripts in different tissues and embryogenesis, the quantitative real-time RT-PCR was employed. Turbot *grim-19* mRNA was widely distributed in all 11 examined tissues with higher levels in brain, liver, head kidney and gill (Fig. 4A). As well, turbot *grim-19* was constitutively expressed in embryogenesis from multicellular to

alevin stage with the highest expression level at gastrula stage (Fig. 4B).

In further, qRT-PCR revealed that *grim-19* expression was induced by several folds in *V. anguillarum* and LCDV challenge tissues. In *V. anguillarum* infected turbot, *grim-19* relative expression reached a maximum value at 12 h in liver (~2.05-fold), 24 h in spleen (~2.65-fold) and 24 h in kidney (~1.96-fold) (Fig. 5). After LCDV challenge, *grim-19* relative expression level was highest at 48 h in liver (~2.02-fold), 12 h in spleen (~3.75-fold) and 48 h in kidney (~2.49-fold) (Fig. 6).

3.4. GRIM-19 protein expression, identification and anti-bacterial activity

As shown in Fig. 7A, a GST-fusion protein with approximately 43 kDa appeared in *E. coli* transformed with pGEX-GRIM19 but not pGEX-4T-1 (Fig. 7A). And the largest expression amount of GST-fusion protein is at 3 h after IPTG induction, accounting for 47.5% of the total proteins (Fig. 7A). The following Western-blotting analysis by GST monoclonal antibody confirmed that the
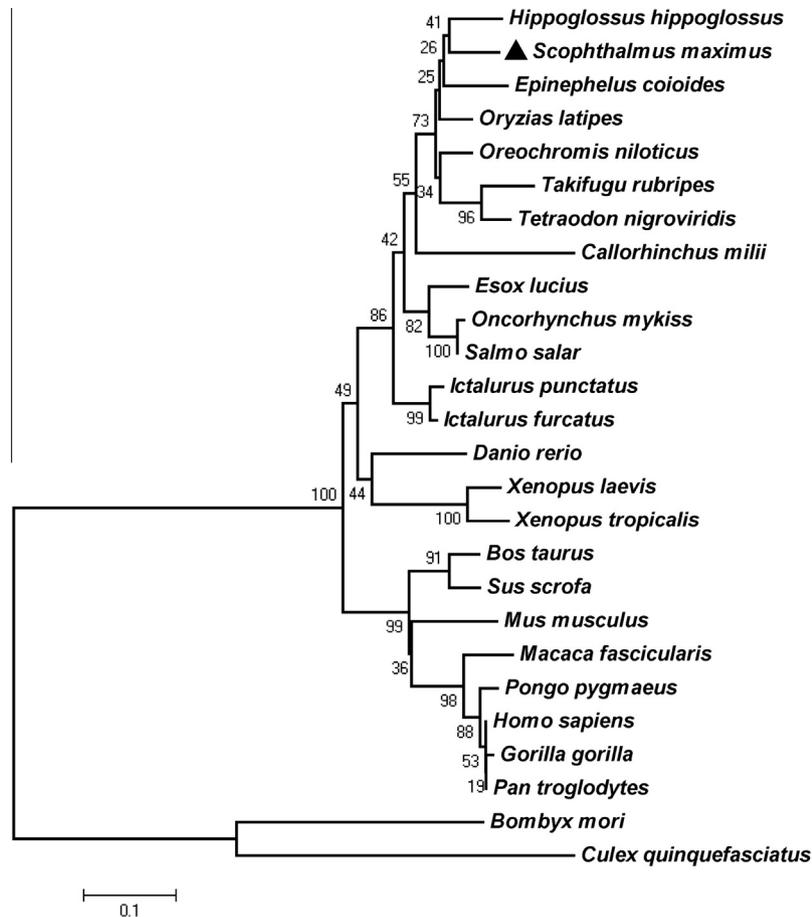
Fig. 3. Phylogenetic analysis of GRIM-19 homologue proteins sequences. A phylogenetic tree was constructed with the neighbor-joining algorithm of MEGA 5.05. The branches were validated by bootstrap analysis from 1000 replications, which were represented by percentage in branch nodes. GRIM19 homologue proteins sequences used in this analysis: silkworm *Bombyx mori* (ABD36198), cattle *Bos taurus* (AAI02407), southern house mosquito *Culex quinquefasciatus* (EDS45017), Australian ghost shark *Callorhinchus milii* (AFK10878.1), rainbow trout *Oncorhynchus mykiss* (ACO08659), Nile tilapia *Oreochromis niloticus* (XP_003438233), Atlantic salmon *Salmo salar* (ACI69466), turbot *Scophthalmus maximus* (ABD61722), pufferfish *Takifugu rubripes* (XP_003975676), green spotted puffer *Tetraodon nigroviridis* (CAG07723), medaka *Oryzias latipes* (XP_004079242), zebrafish *Danio rerio* (AA59474), channel catfish *Ictalurus punctatus* (ADO29400), orange-spotted grouper *Epinephelus coioides* (AFL56355), blue catfish *Ictalurus furcatus* (ADO28292), northern pike *Esox lucius* (ACO14088), western gorilla *Gorilla gorilla* (ABH12254), Atlantic halibut *Hippoglossus hippoglossus* (EU413525), human *Homo sapiens* (AAH09189), crab-eating macaque *Macaca fascicularis* (AB169212), mouse *Mus musculus* (AF286698), common chimpanzee *Pan troglodytes* (ABH12253), bornean orangutan *Pongo pygmaeus* (ABH12255), pig *Sus scrofa* (NP_001231575), western clawed frog *Xenopus tropicalis* (NP_988900), African clawed frog *Xenopus laevis* (ABN58721).

recombinant protein was GST-GRIM19 fusion protein with 43 kDa (Fig. 7B).

In order to detect the anti-bacterial ability of GRIM-19, GST-GRIM19 and GST proteins were purified by GSTrap™ FF column and resolved in ddH$_2$O with 50 and 100 ng/µl. The liquid culture inhibition experiment showed that recombinant GST-GRIM-19 protein could inhibit the growth of *V. anguillarum* in a concentration-dependent manner (Fig. 7C), while no change of *V. anguillarum* was observed in GST or GST-IGF-I proteins treatment experiment.

3.5. The co-localization of GRIM-19 and STAT3 in TK cells

Firstly, the transfection of pCS2-GRIM19-Cherry, which drives the expression of a red fluorescent fusion protein including full-length GRIM19 and Cherry, resulted in clear signals accumulation in the cytoplasm (Fig. 8B). To further analyze the co-localization of GRIM-19 and STAT3, the plasmids pCS2-GRIM19-Cherry and pGFP-STAT3 were co-transfected into TK cells. The results (Fig. 8B) demonstrated that the STAT3-GFP fusion protein and GRIM19-Cherry fusion protein were co-localized in the cytoplasm.

In order to further investigate the subcellular localization of truncated GRIM-19 ORF, plasmids pGFP-GRIM19-ΔN,

pGFP-GRIM19-ΔC and pGFP-GRIM19-ΔN1 carried 41–144, 1–84 and 85–144 amino acids of GRIM-19 were constructed and transfected into TK cells. As shown in Fig. 8C, the similar green fluorescence pattern of pGFP-GRIM19-ΔN and pGFP-GRIM19-ΔC were observed with cytoplasmic distribution, while green fluorescence of pGFP-GRIM19-ΔN1 was distributed in the cytoplasm and nucleus, similar with the GFP pattern of the control pEGFP-N3.

The plasmid pGFP-STAT3-ΔC expressed strong green fluorescence signals in the cytoplasm. However, only little punctate signals were observed in the cytoplasm of TK cells transfected with pGFP-STAT3-ΔN.

3.6. The cell apoptosis function of turbot GRIM-19

In TK and EPC cells, the cell apoptosis were detected after over-expression of p3.1-GRIM19, p3.1-GRIM19△N and p3.1-GRIM19△C. The results (Fig. 9) detected by BD FACSCalibur flow cytometer revealed that the apoptosis rate of TK cells was 21.07% in p3.1-GRIM19 over-expression, 29.54% in p3.1-GRIM19△N over-expression and 26.94% in p3.1-GRIM19△C over-expression. More serious apoptosis were detected in EPC cells with 46.28% in p3.1-GRIM19 over-expression, 63.83% in p3.1-GRIM19△N over-expression and
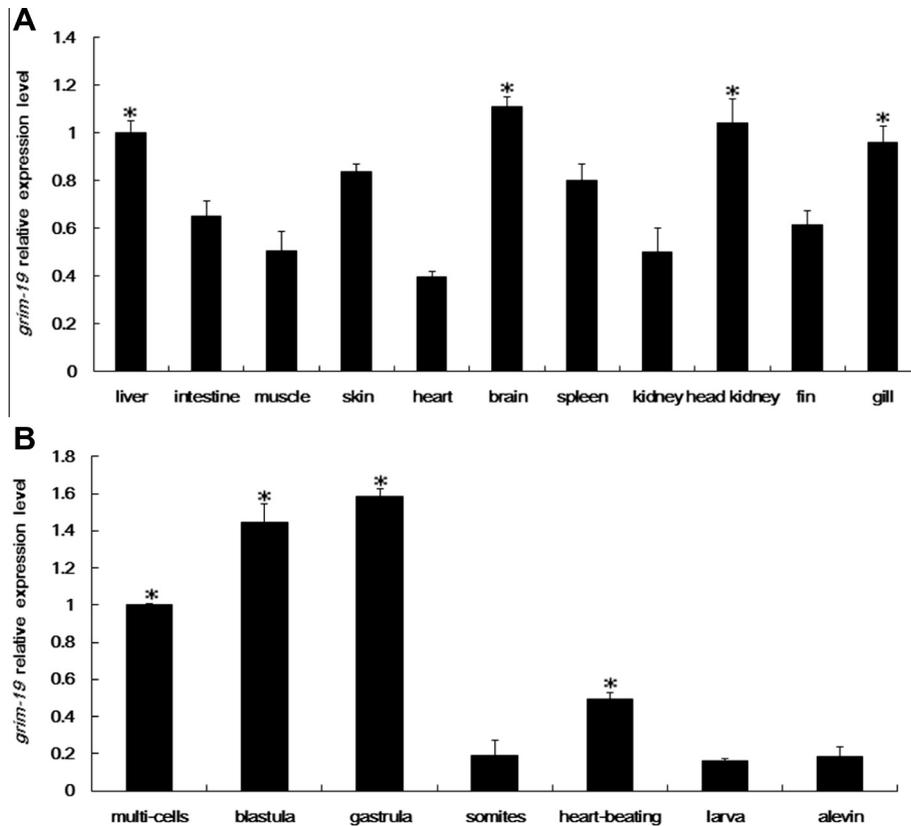
Fig. 4. The expression profiles of turbot GRIM-19 gene in different tissues and embryogenesis. Turbot tissues of liver, intestine, muscle, skin, heart, brain, spleen, kidney, head kidney, fin and gill were harvested. The turbot *grim-19* mRNA expression levels at multi-cells stage, blastula stage, gastrula stage, somites stage, heart-beating stage, larva stage and alevin stage were detected. The expression level was analyzed by $2^{-\triangle\triangle CT}$ method. The *β-actin* gene was used as an internal control to calibrate the cDNA template for all the samples. Vertical bars represented the mean ± S.D. (*n* = 3).
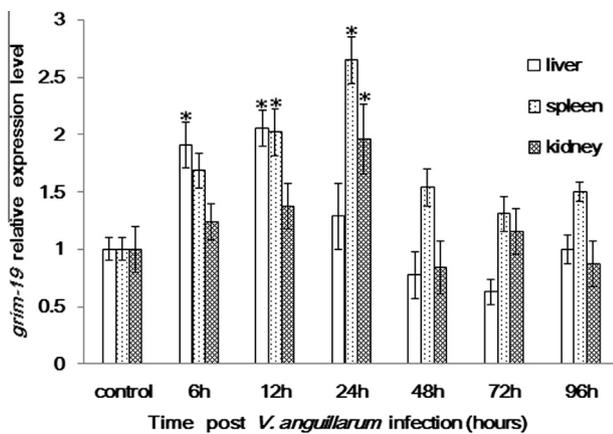

Fig. 5. The quantitative RT-PCR analysis of the expression level of turbot *grim-19* mRNA in liver, spleen and kidney infected with *V. anguillarum*. The turbot *grim-19* mRNA expression levels at 6, 12, 24, 48, 72 and 96 h post injection were examined. Control means the tissues at 12 h after PBS solution injection. *β-Actin* was used as the internal control. Vertical bars represented the mean ± S.D. (*n* = 3).
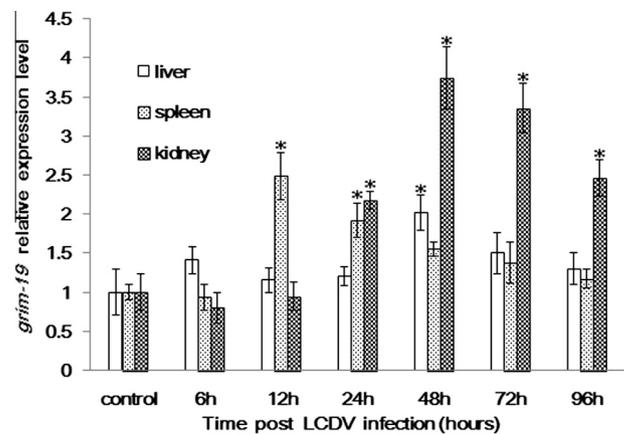

Fig. 6. The quantitative RT-PCR analysis of the expression level of turbot *grim-19* mRNA in liver, spleen and kidney infected with LCDV. The turbot *grim-19* expression levels relative to *β-actin* at 6, 12, 24, 48, 72 and 96 h post injection were examined. Control means the tissues at 12 h after PBS solution injection. All data are expressed as mean ± S.D. (*n* = 3).

41.23% in p3.1-GRIM19△C over-expression. In non-transfection cells and cells transfected with pcDNA3.1, no apoptosis were detected.

3.7. The interaction of GRIM-19 and NF-κB

Whether turbot GRIM-19 participated the NF-κB pathway is investigated by Dual-Luciferase Reporter Assay System with pNFκB-Luc which is designed for measurement of NF-κB activation. The luciferase assay (Fig. 10) showed that the activity of

pNFκB-Luc was induced by overexpression of three plasmids p3.1-GRIM19, p3.1-GRIM19△N and p3.1-GRIM19△C. In addition, the co-transfection of p3.1-GRIM19△N and two luciferase vectors resulted in more significant luciferase activity than p3.1-GRIM19△C and p3.1-GRIM19.

4. Discussion

GRIM-19, a member of GRIMs family, has a wide spectrum of biological activities in innate immunity, cell growth and apoptosis
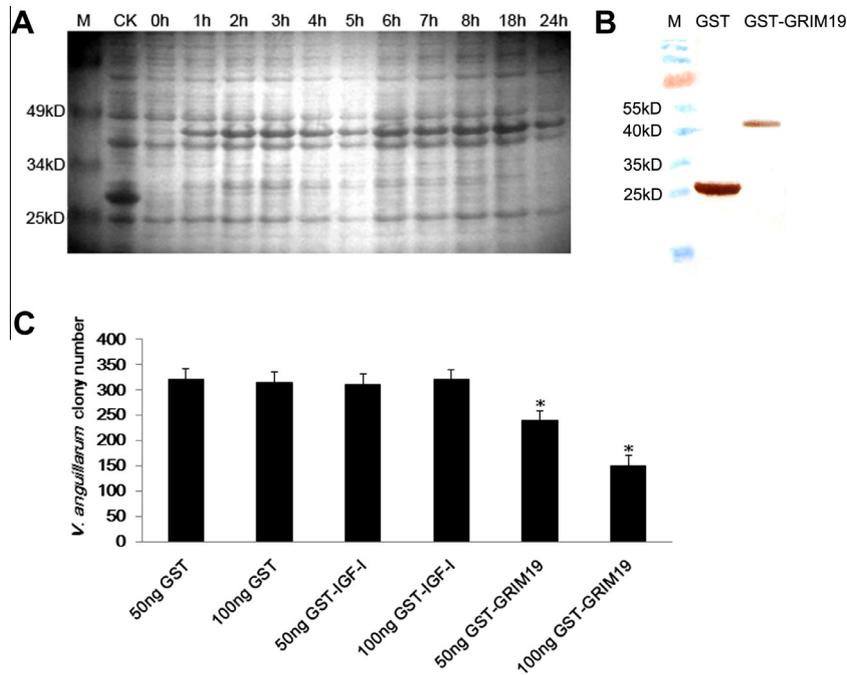
Fig. 7. The GST-GRIM19 expression, identification and ability against to *V. anguillarum*. Part A shows the recombinant GST-GRIM19 expression by SDS–PAGE. M: The protein marker; CK: the expression of the negative control pGEX-4T-1 after 4 h induction by IPTG; 0–24 h: the expression of pGEX-GRIM19 induced by IPTG at 0, 1–8, 18 and 24 h. Part B shows the Western-blot result of GST-GRIM19 and GST proteins detected by the anti-GST antibody. Part C shows the resistance ability of GRIM-19 fused protein to *V. anguillarum*.
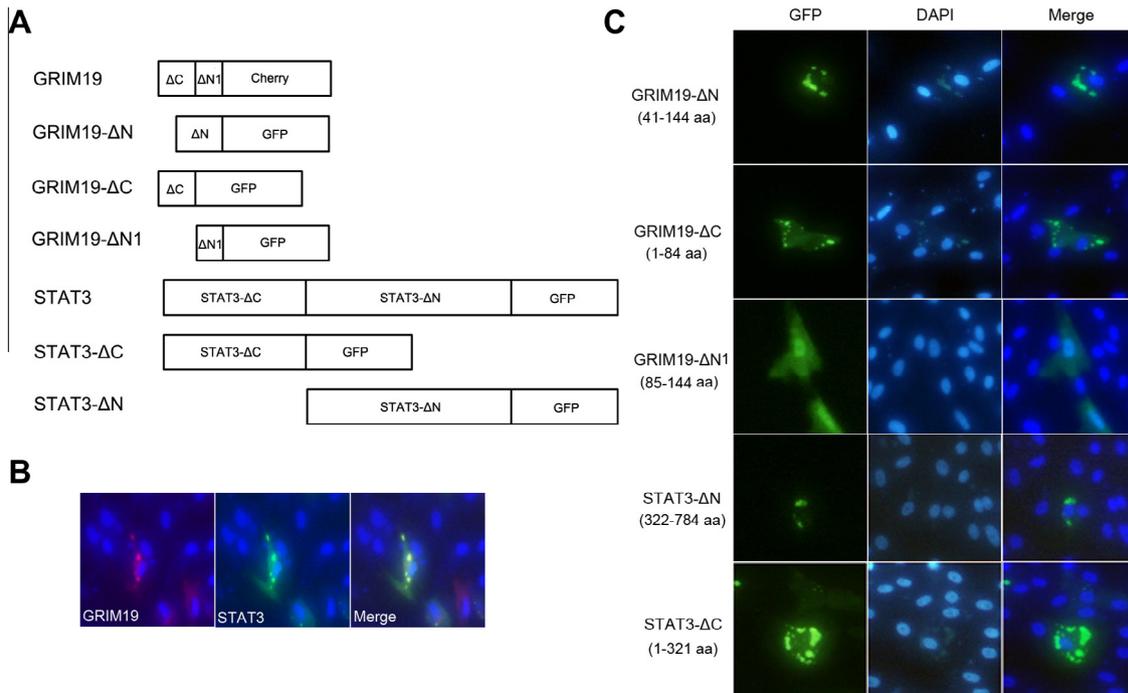

Fig. 8. The subcellular location of turbot GRIM-19 and STAT3 in TK cells. Part A presents a schematic diagram of wild type GRIM19 and STAT3 fluorescence vectors and various truncations. Part B shows the co-localization of STAT3-GFP fusion green fluorescence proteins and GRIM19-Cherry fusion red fluorescence proteins in the cytoplasm of TK cells. Part B shows the fluorescence distribution of pGFP-GRIM19-ΔN, pGFP-GRIM19-ΔC, pGFP-GRIM19-ΔN1, pGFP-STAT3-ΔN and pGFP-STAT3-ΔC in TK cells. The green fluorescence of pGFP-GRIM19-ΔN and pGFP-GRIM19-ΔC were observed in the cytoplasm, while green fluorescence of pGFP-GRIM19-ΔN1 was distributed in the cytoplasm and nucleus. The pGFP-STAT3-ΔC expressed strong green fluorescence signals in the cytoplasm. However, only little punctate signals were observed in the cytoplasm of TK cells transfected with pGFP-STAT3-ΔN.

process (Angell et al., 2000; Kalvakolanu, 2004). In present study, the cloning and characterization of turbot GRIM-19 is described for the first time.

Turbot GRIM-19 cDNA is a 595 bp gene encoding a protein of 144 amino acids, which shares 44%-91% identity to the corresponding sequences of GRIM-19 or NDUFA13 in NCBI database. Multiple
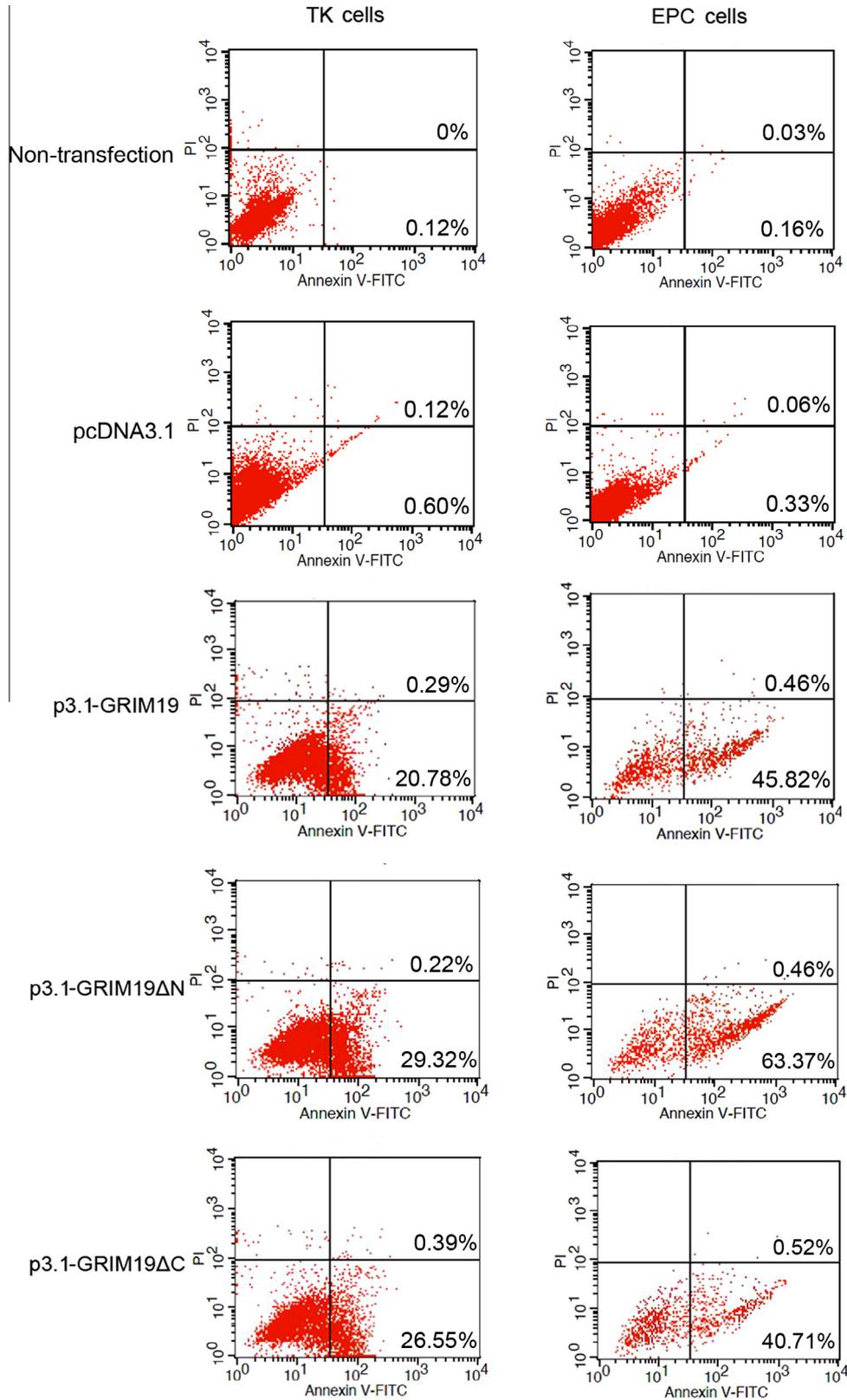
Fig. 9. The cell apoptosis induction in TK and EPC cells by GRIM-19 plasmids. The cells treated with the three GRIM-19 plasmids transfection and LCDV infection were applied for flow cytometric analysis. Annexin-V−/PI− cells, Annexin-V+/PI− cells and Annexin-V+/PI+ cells are live cells, early apoptotic cells, and late apoptotic cells, respectively.

sequences alignment revealed that the N-terminal 35 amino acids are highly conserved in GRIM-19 homologues in human, mouse, cattle, pig, rainbow trout, Atlantic salmon, zebrafish, orange-spotted grouper, Nile tilapia, turbot and so on. Phylogenetic analysis indicated that turbot GRIM-19 deduced amino acids sequence clustered with other fish and frog GRIM-19 homologues to form a distinct clade. All these data suggest that the sequence cloned in present study is the true homologue of turbot GRIM-19.
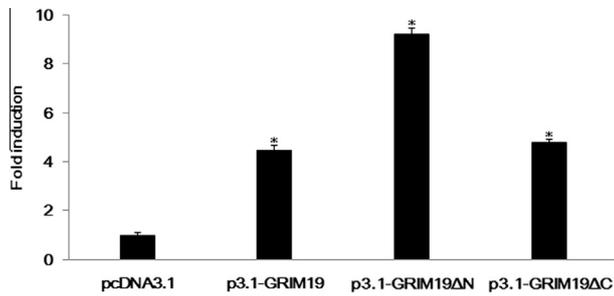
Fig. 10. Activation of pNFκB-Luc by three GRIM-19 plasmids. TK cells were transfected with 0.3 μg pNFκB-Luc, 0.03 μg pRL-TK, and 0.3 μg GRIM-19 plasmids or pcDNA3.1 in each well of 24-well plates. After LCDV infection, the treated cells were harvested for detection of luciferase activity.

Similar with human *grim-19* (Angell et al., 2000), turbot *grim-19* is also constitutively expressed in various tissues, with higher levels in brain, liver, head kidney and gill. It implied that turbot GRIM-19 was involved in turbot normal biological process. In GRIM-19$^{-/-}$ mice, an impaired growth of inner cell mass and trophoblast are observed in blastocysts (Huang et al., 2004), indicating the essential function of GRIM-19 in early embryonic development. Accordingly, the constitutive expression of *grim-19* during turbot embryonic developmental stages revealed that turbot *grim-19* may participate in embryogenesis.

In human colon adenocarcinoma cell line (Caco-2), *S. typhimurium* infection increased *grim-19* mRNA expression with 2.26-fold (Barnich et al., 2005). In human monocytes, exposure to *Porphyromonas gingivalis* led to the up-regulation of GRIM-19 protein with 2.44-fold (Zhou and Amar, 2006). With similar response, in turbot liver, spleen and kidney tissues, *grim-19* expression is also up-regulated by *V. anguillarum* stimulation with 1.96–2.65-fold.

Furthermore, the recombinant turbot GRIM-19 protein could exhibit the resistance ability to *V. anguillarum* by inhibit its growth in a concentration dependent manner, which is consistent with the finding of GRIM-19 protect Caco-2 cells by reducing the intracellular survival of *S. typhimurium* (Barnich et al., 2005).

About the subcellular location of GRIM-19, there are contradictory results in previous study. The studies in Hela (human cervical carcinoma endothelial cells) showed that GRIM-19 protein primarily located in the nucleus with some punctate cytoplasmic distribution (Angell et al., 2000; Zhang et al., 2004). While the studies in several cell line types including Hela, MCF-7 (human breast carcinoma endothelial cells), COS-1 (monkey kidney fibroblasts cells), PC12 (rat neuronal pheochromocytoma cells), H9C2 (rat embryonic myoblasts cells) and FHM (fathead minnow cells) revealed that GRIM-19 protein was exclusively localized in the cytoplasm (Huang et al., 2004; Shi et al., 2013). Other report in HSC3 (human oral squamous cell carcinoma cells) indicated that the majority of GRIM-19 protein was found in the mitochondrion with some nuclear fluorescence (Nallar et al., 2010). In present study, GRIM-19 protein is observed with cytoplasmic distribution in TK cells. In addition, transfection of plasmids pGFP-GRIM19-△N and pGFP-GRIM19-△C results in similar cytoplasmic distribution with the full-length GRIM-19 subcellular location, which indicated that the deletion of N terminal 40 or C terminal 60 amino acids did not affect GRIM-19 cytoplasmic distribution. The subcellular location of another GRIM-19 truncated ORF plasmid pGFP-GRIM19-△N1 is same with that of the control pEGFP-N3. These results suggested that amino acids 41–84 sequences are essential for turbot GRIM-19 cytoplasmic location. Different with this, amino acids 20–30 and 40–60 of human GRIM-19 (Lu and Cao, 2008) or amino acids 30–50 of orange-spotted grouper GRIM-19 (Shi et al., 2013) are responsible for mitochondrial localization.

The co-localization of GRIM-19 and STAT3 in the cytoplasm of TK cells is observed in present study, which indicated the possible interaction of GRIM-19 and STAT3 may be worth to explore in fish like mammalian (Lufei et al., 2003; Zhang et al., 2003). About the interaction region of two proteins, Zhang et al. (2003) found that the transactivation domain (C terminal 83 amino acids) of STAT3 was required for GRIM-19 binding, while Lufei et al. (2003) revealed that the coiled-coil region (amino acids 130–320), DNA-binding and linker domains (amino acids 320–585) of STAT3 were capable of binding to GRIM-19. In our experiment, the subcellular location of truncation mutants of STAT3 suggested that amino acids 1–321 (STAT_int and STAT_alpha domain) (Wang et al., 2011) may be the main determination region for the cytoplasmic co-localization with GRIM-19.

As a cell death regulatory gene, GRIM-19 can cause cell apoptosis to remove the infected or destructed intestinal epithelial cells in response to infection (Barnich et al., 2005). In cancer cells, GRIM-19 plays an important role in inhibiting tumor migration and promoting apoptosis (Tripathy et al., 2010; Huang et al., 2010; Zhou et al., 2011). Turbot GRIM-19 also participated in cell apoptosis regulation process in virus-infected TK cells and EPC cells, with more serious cell apoptosis in EPC cells, which suggested that GRIM-19 may be more effective in tumor cells. More serious apoptosis in p3.1-GRIM19△N transfected cells indicated that functional domains related to apoptosis may be located in the C terminal 60 amino acids of GRIM-19. By sequences analysis, the putative ATP binding domain (VMKDVPGWKVGE) is found in turbot 97–108 amino acids, which has been shown to be essential for cell death induction in human GRIM-19 (Angell et al., 2000).

Previous studies revealed that GRIM-19 involved in NF-κB pathway to regulate immune response (Barnich et al., 2005; Park et al., 2004). In present study, luciferase reporter assay showed that turbot GRIM-19 may also participate in NF-κB pathway. In addition, more significant luciferase activity induced by p3.1-GRIM19△N indicated that the C terminal 60 amino acids of GRIM-19 may be more essential for NF-κB activity.

5. Conclusions

In summary, the cloning and identification of GRIM-19, an important cell death regulatory gene, from turbot are described for the first time. The function of GRIM-19 in turbot immune response and cell apoptosis are revealed, although the intrinsic mechanism remains to be explored further. Also, the anti-bacterial activity of turbot GRIM-19 may be helpful for the development of fish disease-resistant gene products. The detailed interaction research of GRIM-19 with STAT3 or other proteins will provide more comprehensive basis for molecular disease-resistant breeding in aquaculture.

Acknowledgements

References

Angell, J.E., Lindner, D.J., Shapiro, P.S., Hofmann, E.R., Kalvakolanu, D.V., 2000. Identification of GRIM-19, a novel cell death-regulatory gene induced by the interferon-beta and retinoic acid combination, using a genetic approach. J. Biol. Chem. 275, 33416–33426.

Barnich, N., Hisamatsu, T., Aguirre, J.E., Xavier, R., Reinecker, H.C., Podolsky, D.K., 2005. GRIM-19 interacts with nucleotide oligomerization domain 2 and serves

as downstream effector of anti-bacterial function in intestinal epithelial cells. J. Biol. Chem. 280, 19021–19026.

Bromberg, J.F., Wrzeszczynska, M.H., Devgan, G., Zhao, Y., Pestell, R.G., Albanese, C., Darnell Jr., J.E., 1999. Stat3 as an oncogene. Cell 98, 295–303.

Chen, J.X., Li, C.F., Yan, X.H., Li, Yun., Chi, Z.H., Xue, X.W., Wang, Y.G., 2005. Studies on biological characteristics of five pathogenic *Vibrio anguillarum* strains isolated from diseased turbot (*Scophthalmus maximus*) in Shandong province of China. High Technol. Lett. 15, 92–96.

Chen, Y., Lu, H., Liu, Q., Huang, G., Lim, C.P., Zhang, L., Hao, A., Cao, X., 2012. Function of GRIM-19, a mitochondrial respiratory chain complex I protein, in innate immunity. J. Biol. Chem. 287, 27227–27235.

Fan, X.Y., Jiang, Z.F., Cai, L., Liu, R.Y., 2012. Expression and clinical significance of GRIM-19 in lung cancer. Med. Oncol. 29, 3183–3189.

Fearnley, I.M., Carroll, J., Shannon, R.J., Runswick, M.J., Walker, J.E., Hirst, J., 2001. GRIM19, a cell death regulatory gene product, is a subunit of bovine mitochondrial NADH: ubiquinone oxidoreductase (complex I). J. Bio. Chem. 276, 38345–38348.

Fijan, N., Sulimanović, D., Bearzotti, M., Muzinić, D., Zwillenberg, L.O., Chilmonczyk, S., Vautherot, J.F., de Kinkelin, P., 1983. Some properties of the Epithelioma papulosum cyprini (EPC) cell line from carp *Cyprinus carpio*. Ann. Inst. Pasteur. Virol. 134, 207–220.

Huang, G., Lu, H., Hao, A., Ng, D.C., Ponniah, S., Guo, K., Lufei, C., Zeng, Q., Cao, X., 2004. GRIM-19, a cell death regulatory protein, is essential for assembly and function of mitochondrial complex I. Mol. Cell. Biol. 24, 8447–8456.

Huang, Y., Yang, M., Yang, H., Zeng, Z., 2010. Upregulation of the GRIM-19 gene suppresses invasion and metastasis of human gastric cancer SGC-7901 cell line. Exp. Cell Res. 316, 2061–2070.

Kalvakolanu, D.V., 2004. The GRIMs: a new interface between cell death regulation and interferon/retinoid induced growth suppression. Cytokine Growth Factor Rev. 15, 169–194.

Lindner, D.J., Borden, E.C., Kalvakolanu, D.V., 1997. Synergistic antitumor effects of a combination of interferons and retinoic acid on human tumor cells in vitro and in vivo. Clin. Cancer Res. 3, 931–937.

Lu, H., Cao, X., 2008. GRIM-19 is essential for maintenance of mitochondrial membrane potential. Mol. Biol. Cell 19, 1893–1902.

Lufei, C., Ma, J., Huang, G., Zhang, T., Novotny-Diermayr, V., Ong, C.T., Cao, X., 2003. GRIM-19, a death-regulatory gene product, suppresses Stat3 activity via functional interaction. EMBO J. 22, 1325–1335.

Máximo, V., Lima, J., Soares, P., Silva, A., Bento, I., Sobrinho-Simões, M., 2008. GRIM-19 in health and disease. Adv. Anat. Pathol. 15, 46–53.

Meng, L., Chen, S.L., Liu, Y., 2009. Construction of a cDNA library from spleen of *Scophthalmus maximus* and identification of immune-related genes by EST sequencing. J. Fish. China 33, 713–718.

Moore, D.M., Kalvakolanu, D.V., Lippman, S.M., Kavanagh, J.J., Hong, W.K., Borden, E.C., Paredes-Espinoza, M., Krakoff, I.H., 1994. Retinoic acid and interferon in human cancer: mechanistic and clinical studies. Semin. Hematol. 31, 31–37.

Nallar, S.C., Kalakonda, S., Sun, P., Ohmori, Y., Hiroi, M., Mori, K., Lindner, D.J., Kalvakolanu, D.V., 2010. Identification of a structural motif in the tumor-suppressive protein GRIM-19 required for its antitumor activity. Am. J. Pathol. 177, 896–907.

Nishizawa, T., Savas, H., Isidan, H., Ustündağ, C., Iwamoto, H., Yoshimizu, M., 2006. Genotyping and pathogenicity of viral hemorrhagic septicemia virus from free-living turbot (*Psetta maxima*) in a Turkish coastal area of the Black Sea. Appl. Environ. Microbiol. 72, 2373–2378.

Park, H.S., Jung, H.Y., Park, E.Y., Kim, J., Lee, W.J., Bae, Y.S., 2004. Cutting edge: direct interaction of TLR4 with NAD(P)H oxidase 4 isozyme is essential for lipopolysaccharide-induced production of reactive oxygen species and activation of NF-kappa B. J. Immunol. 173, 3589–3593.

Seo, T., Lee, D., Shim, Y.S., Angell, J.E., Chidambaram, N.V., Kalvakolanu, D.V., Choe, J., 2002. Viral interferon regulatory factor 1 of Kaposi's sarcoma-associated herpesvirus interacts with a cell death regulator, GRIM19, and inhibits interferon/retinoic acid-induced cell death. J. Virol. 76, 8797–8807.

Shi, C.Y., Wang, Y.G., Yang, S.L., Huang, J., Wang, Q.Y., 2004. The first report of an iridovirus-like agent infection in farmed turbot *Scophthalmus maximus* in China. Aquaculture 236, 11–25.

Shi, Y., Zhao, Z., Zhu, X., Chen, K., Zhang, Q., 2013. Expression and functional characterization of a gene associated with retinoid-interferon-induced mortality 19 (GRIM-19) from orange-spotted grouper (*Epinephelus coioides*). Fish Shellfish Immunol. 34, 273–279.

Tamura, K., Peterson, D., Peterson, N., Stecher, G., Nei, M., Kumar, S., 2011. MEGA5: Molecular evolutionary genetics analysis using maximum likelihood, evolutionary distance, and maximum parsimony methods. Mol. Biol. Evol. 28, 2731–2739.

Tripathy, M.K., Ahmed, Z., Ladha, J.S., Mitra, D., 2010. The cell death regulator GRIM-19 is involved in HIV-1 induced T-cell apoptosis. Apoptosis 15, 1453–1460.

Wang, N., Wang, X.L., Sha, Z.X., Tian, Y.S., Chen, S.L., 2010. Development and characterization of a new marine fish cell line from turbot (*Scophthalmus maximus*). Fish Physiol. Biochem. 36, 1227–1234.

Wang, N., Yang, C.G., Sun, Z.Z., Wang, X.L., Chen, S.L., 2011. Signal transducer and activator of transcription 3 (STAT3) homologue in turbot (*Scophthalmus maximus*): molecular characterization and expression analysis. Fish Shellfish Immunol. 30, 255–262.

Yu, H., Pardoll, D., Jove, R., 2009. STATs in cancer inflammation and immunity: a leading role for STAT3. Nat. Rev. Cancer 9, 798–809.

Zhang, J., Yang, J., Roy, S.K., Tininini, S., Hu, J., Bromberg, J.F., Poli, V., Stark, G.R., Kalvakolanu, D.V., 2003. The cell death regulator GRIM-19 is an inhibitor of signal transducer and activator of transcription 3. Proc. Natl. Acad. Sci. U.S.A. 100, 9342–9347.

Zhang, L., Gao, L., Li, Y., Lin, G., Shao, Y., Ji, K., Yu, H., Hu, J., Kalvakolanu, D.V., Kopecko, D.J., Zhao, X., Xu, D.Q., 2008. Effects of plasmid-based Stat3-specific short hairpin RNA and GRIM-19 on PC-3M tumor cell growth. Clin. Cancer Res. 14, 559–568.

Zhang, X., Huang, Q., Yang, Z., Li, Y., Li, C.Y., 2004. GW112, a novel antiapoptotic protein that promotes tumor growth. Cancer Res. 64, 2474–2781.

Zhao, X.J., Chen, S.L., Wang, N., Wang, X.L., Xing, S.C., 2010. Cloning, recombinant expression and purification of turbot (Scophthalmus maximus) mature IGF-1. J. Fish. China 34, 1–7.

Zhou, Q., Amar, S., 2006. Identification of proteins differentially expressed in human monocytes exposed to *Porphyromonas gingivalis* and its purified components by high-throughput immunoblotting. Infect. Immun. 74, 1204–1214.

Zhou, Y., Wei, Y., Zhu, J., Wang, Q., Bao, L., Ma, Y., Chen, Y., Feng, D., Zhang, A., Sun, J., Nallar, S.C., Shen, K., Kalvakolanu, D.V., Xiao, W., Ling, B., 2011. GRIM-19 disrupts E6/E6AP complex to rescue p53 and induce apoptosis in cervical cancers. PLoS One 6, e22065.